Structural Replacement of Active Site Monovalent Cations by the ϵ-Amino Group of Lysine in the ATPase Fragment of Bovine Hsc70[†,‡]

Sigurd M. Wilbanks[§] and David B. McKay*

Beckman Laboratories for Structural Biology, Department of Structural Biology, Stanford University School of Medicine, Stanford, California 94305-5400

Received December 11, 1997; Revised Manuscript Received March 26, 1998

ABSTRACT: We have assessed the ability of the ϵ-amino group of a non-native lysine chain to substitute for a monovalent cation in an enzyme active site. In the bovine Hsc70 ATPase fragment, mutation of cysteine 17 or aspartic acid 206 to lysine potentially allows the replacement of an active site potassium ion with the ϵ-amino nitrogen. We examined the ATP hydrolysis kinetics and crystal structures of isolated mutant ATPase domains. The introduced ϵ-amino nitrogen in the C17K mutant occupies a significantly different position than the potassium ion. The introduced ϵ-amino nitrogen in the D206K mutant occupies a position indistinguishable from that of the potassium in the wild-type structure. Each mutant retains $<5\%$ ATPase activity when compared to the wild type under physiological conditions (potassium buffer) although substrate binding is tighter, probably as a consequence of slower release. It is possible to construct a very good structural mimic of bound cation which suffices for substrate binding but not for catalytic activity.

Hsc70[1] is a molecular chaperone of the 70 kilodalton heat shock protein family. It comprises separable ATP hydrolytic and peptide binding activities (*1*, *2*). Potassium is required for ATP hydrolysis and proper regulation of peptide binding and release (*3*, *4*). The basis of the requirement is a pair of potassium ions specifically bound in the ATP hydrolytic site on either side of the scissile bond (*5*). The potassium ions interact with the β- and γ-phosphate moieties of the bound nucleotide, suggesting that they may participate directly in establishing the transition state geometry for nucleotide hydrolysis. One of the ions is positioned to mimic the function of the lysine ϵ-amino group of the Walker "P-loop" motif of other phosphoryl-transferases.

The catalytic activities of a significant number of enzymes, including many phosphoryl-transferases, display monovalent ion dependence, often with potassium supporting maximal activity [see (*6*) for review]. Additionally, there is crystallographic evidence for the direct involvement of potassium in phosphoryl transfer by pyruvate kinase (*7*) and fructose-1,6-bisphosphatase (*8*). In the former case, the potassium requirement can be relieved by an introduced lysine residue (*9*), while in the latter case potassium appears to be interchangeable with a native arginine guanidinium group. In this context, we wished to determine to what extent a positive charge from a protein side chain can substitute structurally and functionally for each of the potassium ions in the Hsc70 active site. The ionic radius of the ammonium ion (1.48 Å), and, by implication, that of a primary amino group, is much closer to that of the potassium ion (1.33 Å) than that of sodium (0.96 Å) (*10*).

Actin has an ATPase activity and is structurally homologous to the ATPase domain of Hsc70 (*11*, *12*). Superposition of the X-ray crystal structures of actin and Hsc70 shows that the interactions with ATP are almost identical. However, the potassium ion at site 1 of Hsc70 appears to be replaced by the ϵ-amino group of lysine 18 in actin. The main-chain atoms and β carbon of actin lysine 18 correspond to those of Hsc70 cysteine 17. Molecular modeling suggested that mutation of Hsc70 cysteine 17 to lysine could place the mutant side chain in a position like that of actin's lysine 18.

Inspection of the Hsc70 model suggested that a similar substitution of a protein side chain could be made in the other potassium site (site 2) by creating D206K. One carboxylate oxygen of aspartic acid 206 coordinates potassium in the native structure and is expected to be charged, so this change should result in net charge gain in the active site. The other carboxylate oxygen of D206 has no direct interactions with substrate, bound ions, or protein atoms. The interactions made by the potassium ions at sites 1 and 2 are diagrammed in Figure 1, and the position of cysteine 17 is indicated.

We constructed C17K and D206K mutants of the Hsc70 ATPase domain and tested their hydrolytic rates and nucleotide binding abilities. We also constructed and tested C17R and D206R mutants in an alternative strategy to substitute

[†] This work was supported by Grant GM-39928 from the National Institutes of Health (to D.B.M.) and by the resources of the Beckman Laboratories for Structural Biology.

[‡] Coordinates for the models of the ATPase domains have been deposited in the Brookhaven Protein Data Bank with entry numbers 1BA1 for mutant C17K and 1BAϕ for mutant D206K.

* To whom correspondence should be addressed at the Department of Structural Biology, Sherman Fairchild Building, Stanford University School of Medicine, Stanford, CA 94305-5400. Telephone: (650) 723-6589. FAX: (650) 723-8464.

[§] Current address: Biochemistry Department, University of Otago, Box 56, Dunedin, New Zealand.

[1] Abbreviations: Hsc70, 70 kDa heat shock cognate protein; Hsp70, 70 kDa heat shock protein; HEPES, *N*-(2-hydroxyethyl)piperazine-*N*′-2-ethanesulfonic acid; MOPS, 3-(*N*-morpholino)propanesulfonic acid; CHES, 2-(*N*-cyclohexylamino)ethanesulfonic acid; PEG-8000, poly(ethylene glycol) of approximate molecular weight 8000.

S0006-2960(97)03046-8 CCC: $15.00
Published on Web 04/30/1998

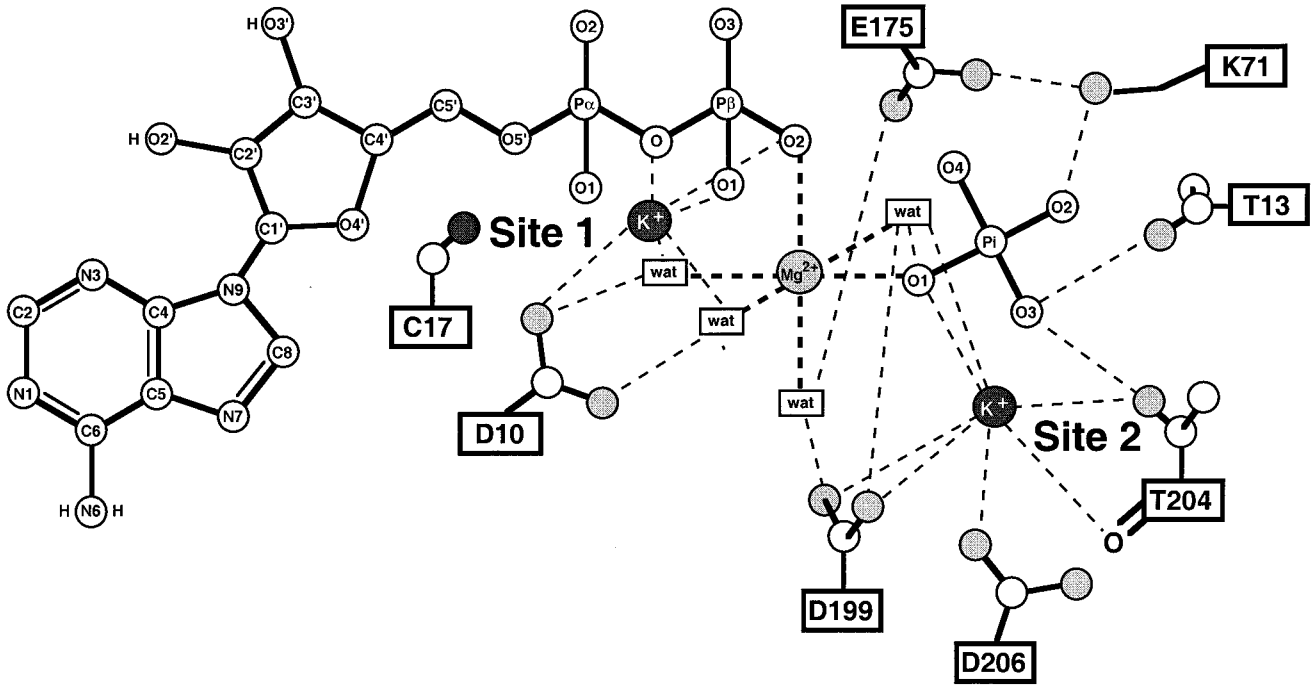

FIGURE 1: Schematic diagram of the wild-type active site with MgADP and potassium bound. The coordination of magnesium and the environment of the potassium ions are emphasized. Nucleotide, selected residues, and solvent molecules are shown and labeled. Potassium ions are darkly shaded; magnesium and the oxygen and nitrogen atoms of protein side chains are lightly shaded. Selected noncovalent interactions are indicated by dashed lines. Based on references (*23*, *5*).

basic side chains for potassium. In addition, we solved the crystal structures of C17K and D206K to assess the location and interactions of the lysine ϵ-amino nitrogens.

MATERIALS AND METHODS

Mutagenesis. The single-residue mutations C17K, C17R, D206K, and D206R were introduced individually by single-stranded mutagenesis (Mutagene kit, Biorad, Richmond, CA) into the coding sequence for the Hsc70 ATPase fragment in a pET-based expression plasmid. This expression plasmid was prepared by introduction of a 1170 base pair *Nde*I−*Sal*I fragment from our pT7-7-based Hsc70 expression plasmid into pET-21a(+) cut with the same enzymes (*13*). Mutagenic primers were complementary to the coding strand (mismatches are underlined): C17K, 5′-GGAAGACAC-CAACTTTAGAATAGGTGG-3′; C17R, 5′-GGAAGACAC-CAACGCGAGAATAGGTGG-3′; D206K, 5′-GGATTGA-CATTTAAAAGTGCCACCC-3′; D206R, 5′-CCTCAATAG-TGAGAATCGATACACGAAAAGTGCCACCC-3′. Mutations were identified by restriction analysis for (D206K and D206R) and confirmed by sequencing ~200 base pairs surrounding the mutations.

Protein Expression and Purification. Recombinant mutant ATPase domain proteins were prepared using methods previously described (*14*, *13*). Briefly, proteins were expressed in *E. coli* and purified by anion exchange chromatography (Q-sepharose, Pharmacia, Uppsala, Sweden), affinity chromatography (ATP−agarose; Sigma, St. Louis, MO), chromatofocusing (MonoP; Pharmacia), and gel-filtration (Superdex75, Pharmacia).

Pre-Steady-State ATP Hydrolytic Kinetic Measurements. ATP hydrolysis was assessed by thin-layer chromatography, essentially as published (*14*). For time points at greater than 20 min, reactions were not acid-quenched prior to chromatography, but analyzed immediately after time points were collected. Potassium buffer was 10 mM MOPS (pH 7)/150 mM KCl/4.5 mM $Mg(CH_3COO)_2$. Sodium buffer was the same, except that NaCl replaced KCl.

Nucleotide Binding and Release. All experiments were performed at 25 °C. [α-^{32}P]ADP was prepared by Dr. J.-H. Ha as published, and the ADP release rate was measured as published (*15*). It was possible to directly measure the interaction of ATP with the mutant fragments as release is >5-fold faster than hydrolysis. Equilibrium binding constants (K_D) and release rates (k_{off}) of ATP were measured by the method used for ADP with w.t. protein (*15*). The rate of ATP binding (k_{on}) was calculated as the ratio of k_{off} and K_D.

Crystallization and Data Collection. Crystals of D206K and C17K mutant proteins were grown essentially as described (*16*) from 20% PEG-8000, 1.0 M NaCl, 50 mM CHES adjusted to pH 9 with NaOH, with 1 mM MgATP, and with 6 mg/mL protein; the crystals were isosymmetric with those obtained previously (space group $P2_12_12_1$). Since crystallization is dependent on seeding, small crystals of wild-type protein were used initially to seed mutant protein crystallizations. The resulting crystals were then crushed and used as seeds in a third round of crystallization. Crystals were adapted to a cryosolvent that allows flash-freezing. Crystals of the D206K mutant were initially shifted to 5% ethylene glycol/20% PEG-8000/1.0 M NaCl/40 mM CHES (adjusted to pH 7.0 with NaOH) and then to progressively higher ethylene glycol (10%, 15%, 20%) in the same mother liquor. Crystals were soaked ~10 min at each intermediate ethylene glycol concentration. The procedure for C17K was identical except that the synthetic mother liquor contained 50 mM HEPES, pH 7, in place of CHES.

Table 1: Crystallographic Data Collection, Reduction, and Model Refinement

	C17K	D206K
Data Collection		
unit cell		
a (Å)	143.8	143.3
b (Å)	64.1	63.8
c (Å)	46.1	46.5
max resolution (Å)	1.7	1.9
observations	138386	102051
unique reflections	45230	34106
completeness	0.947	0.989
R_{sym}[a]	0.051	0.056
Refinement		
rigid body refinement translation (Å)	0.02	0.35
rigid body refinement rotation (deg)	1.7	4.2
final resolution used in refinement	6.0↔1.7	8.0↔1.9
reflections used in refinement	39566	29809
reflections in test set	4454	3357
$R_{crystallographic}$[b] (highest res. bin)	0.202 (0.396)	0.216 (0.297)
R_{free}[b] (highest res. bin)	0.244 (0.440)	0.275 (0.312)
water molecules modeled	446	424
rms[c] bond deviation from ideal (Å)	0.006	0.007
rms[c] angle deviation from ideal (deg)	1.3	1.3

[a] $R_{sym} = \sum|I_i - \langle I\rangle|/\sum\langle I\rangle$ where I = diffraction intensity and $\langle I\rangle$ = mean measured intensity. [b] $R_{crystallographic} = \sum|F_c - F_o|/\sum F_o$ where F_o = observed structure factor amplitude in working set = $|I^{1/2}|$, F_c = structure factor amplitude calculated from model, and R_{free} is the same, using F_o in the test set. [c] rms, root mean square.

A crystal of mutant D206K adapted to 20% ethylene glycol mother liquor at 4 °C was flash-frozen to ~100 K in a stream of cold N_2 gas. Data were collected with a Rigaku R-axis image plate system using CuKα radiation monochromatized with graphite. Data collection parameters were the following: crystal-to-detector distance, 100 mm; detector swing, 10°; oscillation range and exposure time, 1.2° and 48 min when the *a** axis was greater than 30° from direct beam, and 0.7° and 28 min when the *a** axis was less than 30° from direct beam. Crystal orientation and unit cell parameters were determined with the Molecular Structure Corporation's R-axis software. Data were collected from a crystal of mutant C17K using the same procedure, except using an oscillation range of 1.2° and an exposure time of 54 min for all orientations. Data collection statistics are summarized in Table 1.

Model Refinement. Standard crystallographic computations were performed using DENZO (*17*) and CCP4 (*18*). XPLOR (*19*) was used for model refinement by both simulated annealing and positional restrained least-squares minimization. Model building was done with the program CHAIN (Rice version ESVAIN 2.2) on an Evans and Sutherland ESV (*20*).

Our earlier model for wild-type ATPase fragment with MgADP and P_i bound [PDB #1HPM (*5*)] was positioned in the asymmetric unit of the C17K crystal by rigid-body refinement in XPLOR. Bound nucleotide, active site solvent and cations, and mutant side chains were omitted from the model. One cycle of simulated annealing using data from 8 to 1.7 Å reduced the *R* factor to below 0.25.

Multiple rounds of manual, positional, and *B*-factor refinement were used to adjust the protein model and place nucleotide, metal ions (Mg^{2+} or Na^+), and water molecules in well-defined peaks of density found at reasonable distances (2.5−3.1 Å) from polar groups. Automated positional and *B*-factor refinements were carried out with XPLOR. The same procedure was followed for refinement of the D206K mutant protein structure. Refinement statistics are summarized in Table 1.

RESULTS

Initial model building suggested that the positive charge of the side chain of either lysine or arginine placed at amino acid position 17 or 206 might displace K^+ ions 1 or 2, respectively, from the active site of the ATPase fragment of Hsc70. The extent to which the positively charged side chains would mimic the monovalent ion in interactions with the phosphates of ATP, and the extent to which a given substitution would support ATP hydrolysis, was unpredictable. Also, although we could suggest that a localized positive charge of the lysine ϵ-amino group would be a better mimic of the monovalent ion than a positive charge distributed over the guanidinium group of the arginine side chain, the differences between the two substitutions could not be predicted. In this context, we first made mutations substituting both lysine and arginine at positions 17 and 206 and measured their hydrolytic activity.

Purified ATPase fragments of the mutant proteins were analyzed for single-turnover hydrolytic rates, using 30 nM to 10 μM protein (thereby spanning the anticipated K_M of ATP) and ≤1 nM nucleotide. All mutants showed low hydrolytic rates (below 0.0004/s), requiring incubations of hours to observe measurable hydrolysis. Apparent hydrolytic rates (k_{obs}) were computed by fitting a single exponential to the time courses of hydrolysis (e.g., those for D206K are shown in Figure 2). Values for K_M and $k_{hydrolytic}$ were then computed by fitting the expression $k_{obs} = (k_{hydrolytic} \times [protein])/(K_M + [protein])$ to the hydrolytic rates measured as a function of protein concentration. Data are shown in Figure 3, using a (nonconventional) logarithmic scale in order to span the range of conditions used in the measurements.

Results for measurements of C17K and D206K are summarized in Table 2. D206R has hydrolytic rates experimentally indistinguishable from those of D206K. C17R showed no measurable hydrolytic activity. Pre-steady-state kinetic measurements show that all mutants have rates that are less than 4% of the wild-type protein under physiological conditions, i.e., in the potassium buffer. The hydrolytic rates of C17K, D206K, and D206R in sodium buffer are similar to their rates in potassium buffer; further, the rates are of the same order as that of wild-type protein in sodium buffer. It is notable that none of the mutants show the 60-fold rate enhancement in potassium, as compared to sodium, that is measured here for the wild-type protein. The constants measured for w.t. in the presence of potassium are within experimental error of those published earlier [$k_{hydrolytic} = 0.013 \pm 0.003\ s^{-1}$; $K_M = 650 \pm 140$ nM, (*15*)].

The K_M for ATP hydrolysis by the C17K mutant is an order of magnitude lower than for wild type and D206K proteins. This suggested a tighter interaction with nucleotide in the C17K mutant. To determine whether this was the case, nucleotide binding to the mutant fragments was assessed both at equilibrium and under pre-steady-state conditions (Table 2). The K_D (as measured by filter binding) for ATP of each mutant is similar to the K_M inferred

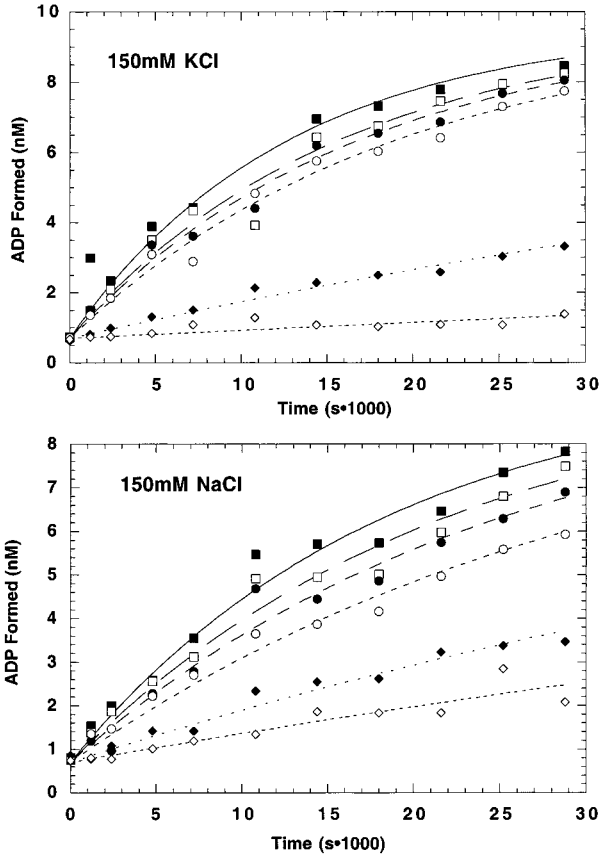

FIGURE 2: Hydrolysis of ATP by Hsc70 D206K ATPase fragment under pre-steady-state conditions. Experiments in the presence of potassium (upper panel) or sodium (lower panel) are shown. Protein concentrations are (■) 10 μM, (□) 3.2 μM, (●) 1 μM, (○) 316 nM, (◆) 100 nM, and (◇) 32 nM. Curves show a single-exponential function fit to the data.

from the hydrolytic measurements. The release of nucleotide is an order of magnitude slower from C17K mutant than from wild-type protein or D206K. The calculated binding rate for ATP is between 2.7 and 12 $\times$ 10^4 for all mutants.

The lysine replacement mutants (C17K and D206K) were chosen for structural analysis, since (i) they both retain hydrolytic activity (albeit it at a low level), while one of the arginine replacements does not, and (ii) model building originally suggested lysine would be a better structural mimic of potassium than arginine in both mutants.

The mutant ATPase domains crystallized under the same conditions as wild-type protein. Statistics for data collection, structure determination by molecular replacement, and model refinement are summarized in Table 1. Positions of mutated side chains and the nucleotide species and occupancy were determined unambiguously from omit maps computed after simulated annealing from 1000 K to 300 K with molecular models lacking these features. The current models include amino acid residues 4−381, 1 ADP, 1 P_i (only in D206K), 1 Mg^{2+} ion, a single Na^+ ion (since 1 of the 2 active-site monovalent ions is displaced in each mutant), 2 Cl^- ions, and ~440 water molecules. The C17K active site shows partial occupancy by ATP, ADP, and P_i. Iterative rounds of occupancy and *B*-factor refinement supported >50% occupancy by ADP, but <50% by ATP and P_i; the active site contents are modeled accordingly. The positions of side chains of a few surface residues could not be determined

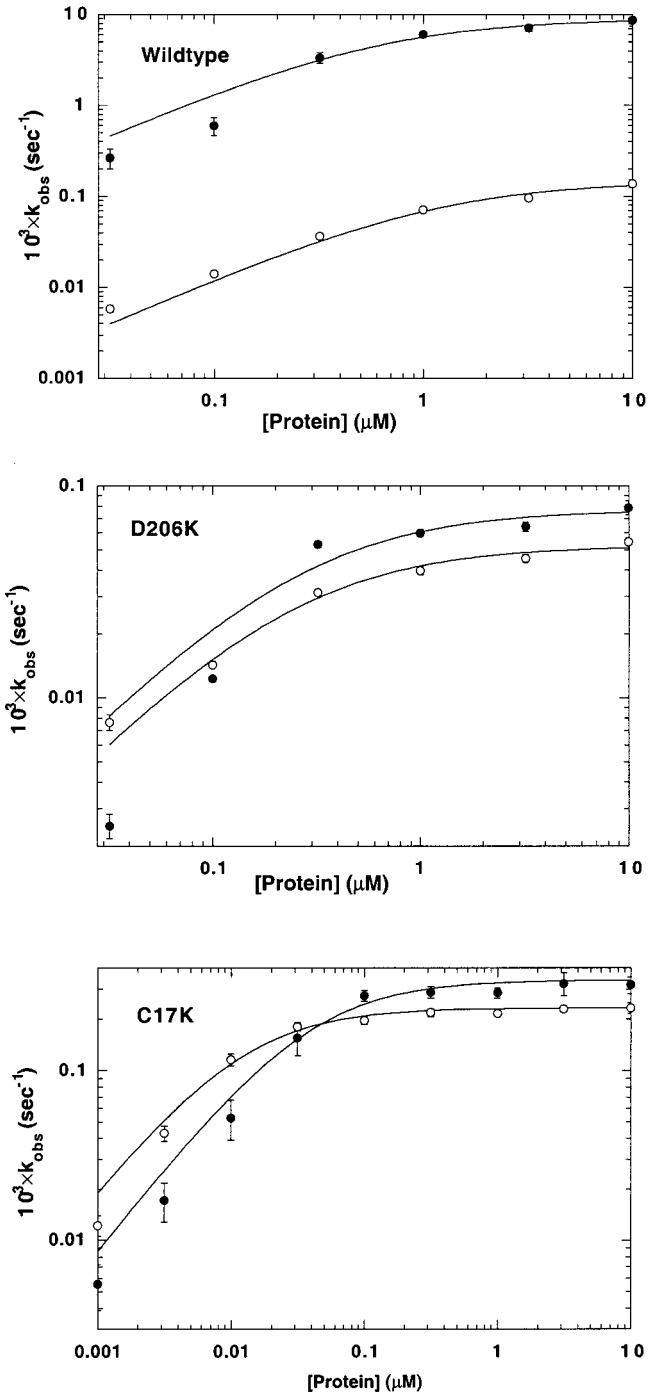

FIGURE 3: Concentration dependence of the apparent hydrolytic rate (kobs) for Hsc70 ATPase fragment. Data in the presence of 150 mM KCl (●) and 150 mM NaCl (○) are shown for wild type (upper panel), D206K (middle panel), and C17K (lower panel). Error bars represent the standard deviation of multiple measurements. Lines show the fit from which kinetic parameters were inferred. *n.b.*: all axes are drawn logarithmically.

and are modeled as alanine. Both structures are indistinguishable from the wild-type molecule in overall tertiary fold (rmsd 0.2 Å computed with α carbons).

The two mutant structures were compared to the structure of the ATPase fragment with MgADP, P_i, and two K^+ ions bound or two Na^+ bound [PDB accession numbers 1HPM and 3HSC, respectively] by superimposing the α-carbon atoms of residues 7−39, 116−174, 193−225, and 306 −353, i.e., the two structural domains which form the nucleotide binding cleft.

Table 2: Kinetic Constants in the Presence of Potassium or Sodium[a]

	wild type	C17K	D206K
$k_{hydrolytic}$ (s^{-1})			
K	0.009 ± 0.001	0.00034 ± 0.00001	0.000076 ± 0.000007
Na	0.00015 ± 0.0001	0.00023 ± 0.00001	0.000052 ± 0.000002
K_M (nM)			
K	600 ± 130	40 ± 10	270 ± 110
Na	1140 ± 260	11 ± 2	250 ± 50
K_D, ATP (nM)			
K	nd	30 ± 10	400 ± 100
Na	nd	50 ± 10	480 ± 80
k_{off}, ATP (s^{-1})			
K	nd	0.0015 ± 0.0006	0.011 ± 0.004
Na	nd	0.0059 ± 0.0014	0.024 ± 0.005
k_{on}, ATP ($s^{-1}M^{-1}$, calcd)			
K	nd	50000 ± 36000	27000 ± 16000
Na	nd	120000 ± 50000	50000 ± 18000
k_{off}, ADP (s^{-1})			
K	0.035 ± 0.007	0.0024 ± 0.0002	nd
Na	nd	0.0023 ± 0.002	nd

[a] Values are from three different determinations at 25 °C. nd = not determined.

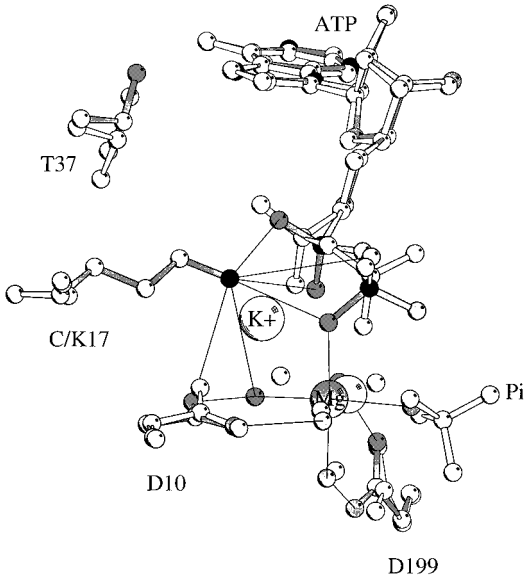

FIGURE 4: Site 1: superposition of the C17K mutant onto wild type with potassium bound. Nucleotide, selected residues, and solvent molecules are shown and labeled. Bound ions are shown as large balls, other atoms as small balls. Selected noncovalent interactions in the mutant structure are indicated by lines. The structure of the mutant is drawn with dark gray bonds and atoms colored as follows: phosphorus and nitrogen in black; magnesium and oxygen in dark gray; carbon in light gray. The structure of wild-type protein with site 1 K^+ is shown as lightly shaded balls-and-sticks. The superposition is described in the text. The orientation is rotated roughly 90° from that of Figure 1. Figures 4−6 were prepared using Molscript (*26*).

In C17K, the ϵ-amino group of lysine 17 sits 1.6 Å away from the position occupied by potassium in site 1 of the wild type (Figure 4). The lysine side chain appears to clash with T37, the Cβ of which is displaced 0.5 Å (and Cα by 0.3 Å) relative to the wild-type structure. The ϵ-amino nitrogen is substantially closer to the α-phosphate and more distant from the β-phosphate of the bound nucleotide, when compared to the K^+ ion in the wild-type structure, and hence it has a different set of interactions with the nucleotide (Table 3). However, those contacts which occur in both structures are of similar length.

Table 3: Interatomic Cation−Oxygen Distances[a]

ligand	Lys ϵ-NH_4	K^+	Na^+
Site 1: Potassium or Sodium in Wild Type vs Lysine ϵ-Amino Group in C17K			
Pα1 oxygen	2.82	(3.92)	(4.25)
Pα2 oxygen	(3.98)	(4.26)	(3.99)
Pα−Pβ oxygen	(3.96)	3.13	(3.64)
Pβ1 oxygen	3.02	3.11	(3.89)
Pβ2 oxygen	(4.11)	3.22	2.40
D10 δ oxygen	(3.64)	2.57	2.54
Y15 carbonyl	2.95	2.58	2.43
+*x* water	(3.54)	2.89	2.71
+*y* water	(4.84)	3.07	3.09
water	(4.87)	2.65	2.32
average	2.93	2.90	2.59
Site 2: Potassium or Sodium in Wild Type vs Lysine ϵ-Amino Group in D206K			
P_i oxygen	2.76	2.78	2.27
Pβ3 oxygen	(4.42)	(4.74)	2.53
D199 δ1 oxygen	2.98	3.24	(4.26)
D199 δ2 oxygen	(3.74)	3.43	(4.56)
D206 δ oxygen	(absent)	2.84	(4.78)
T204 γ oxygen	2.89	2.67	2.29
T204 carbonyl	3.05	3.04	(3.37)
−*y* water	3.28	3.01	2.60
Na^+ assoc water	(absent)	(absent)	2.29
average	3.00	3.00	2.40

[a] Distances are shown in angstroms; those that are substantially larger than normal coordination distances are shown in parentheses for comparison of structures and are not counted toward average values. Distance in wild-type structures and numbering of atoms are as in (*23*).

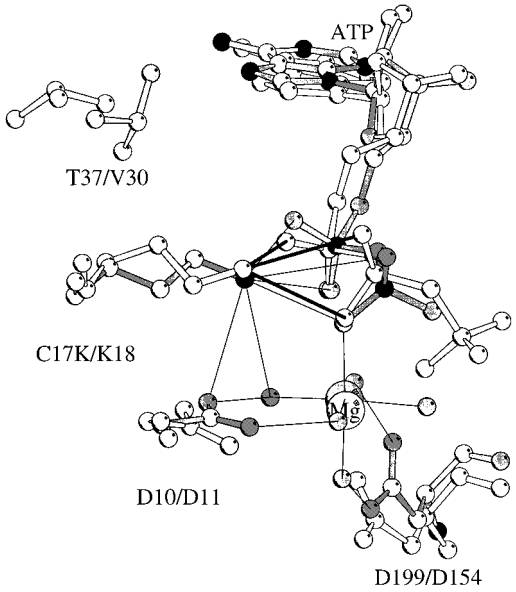

FIGURE 5: Site 1: superposition of the C17K mutant on actin. The orientations mutant Hsc70 residues are as in Figure 4. The structure of actin is shown as lightly shaded balls-and-sticks. Labels identify homologous Hsc70 and actin residues, respectively. Interactions of actin lysine 18 with nucleotide are shown as heavy lines. Superposition was calculated using positions of the C_α atoms in models of the two proteins lacking their relative insertions and deletions.

The position of the ϵ-amino group of lysine 17 is much closer to that of lysine 18 in actin (Figure 5) than it is to the potassium ion bound to wild-type Hsc70. The overall arrangement of the lysine methylenes and the nucleotide phosphates is different. However, three important features are preserved. First, the position of the Hsc70 lysine 17

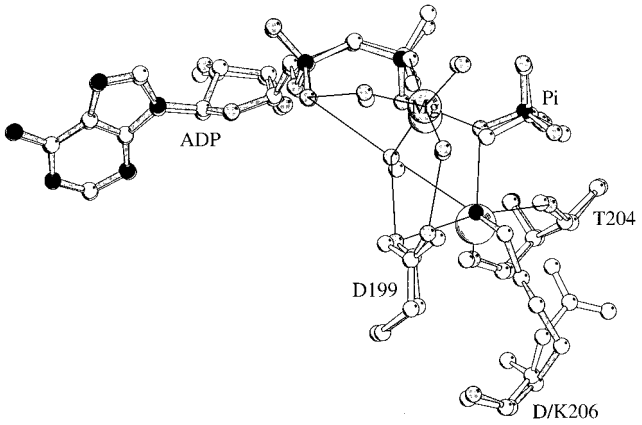

FIGURE 6: Site 2: superposition of the D206K mutant on wild type with bound potassium. Shading scheme and superposition are the same as Figure 4. This view is rotated relative to Figures 4 and 5 and has roughly the orientation of Figure 1. The ϵ-amino nitrogen of the non-native lysine is hidden within the superimposed site 2 potassium ion of the w.t. structure (large ball between D199 and T204), but has been drawn as if exposed.

ϵ-amino nitrogen is similar to that of actin lysine 18; second, in both proteins, the closest interaction of the ϵ-amino group is with the α-phosphate of the bound nucleotide; and third, the homologous residues V37 in actin and T37 in the Hsc70 mutant pack against the lysine methylenes, apparently constraining the side chain position. However, since the structure of actin is known only to 3 Å, the comparison can be only approximate.

In D206K, the ϵ-amino nitrogen of lysine 206 occupies the position of potassium at site 2 in the wild-type protein (0.3 Å distant, Figure 6). It makes essentially the same contacts as does the K^+ ion in the wild-type structure. The only observable difference is a rotation of the D199 carboxyl group to bring a single oxygen closer to the non-native ϵ-amino group of D206K (Table 3).

DISCUSSION

We have substituted positively charged protein side chains for two monovalent ions in the Hsc70 ATPase site. None of the mutations support hydrolysis at the level achieved by the w.t. ATPase domain with potassium bound in the two sites. Since mutation of either cysteine 17 (monovalent ion site 1) or aspartic acid 206 (site 2) alone shows a marked defect, we conclude that potassium is required at both sites for a maximal hydrolytic rate.

Mutations C17K, D206K, and D206R support hydrolytic rates similar to that of the wild-type protein with sodium bound but lack the significant rate enhancement when sodium is replaced with potassium, in sharp contrast to the 60-fold increase seen with wild-type protein. These residual enzymatic activities, along with the crystal structures of mutants C17K and D206K, show that these changes introduce no gross defect in the ATPase domain. In fact, nucleotide binding is tighter to the lysine mutants than to w.t. The small variation of the k_{on} (calculated) for mutants suggests that the mechanism of binding has not been greatly altered in any mutant. The good agreement between K_M and K_D in both lysine mutants indicates that binding is well modeled as a single step. We conclude that the defect which leads to reduced hydrolytic rates in the mutants affects a step after nucleotide binding.

The ϵ-amino group of C17K is neither a good structural mimic nor a sufficient functional replacement. It is displaced >1.5 Å and makes few of the same contacts as the potassium ion (Figure 4). It excludes ions from site 1, accounting for the mutant's insensitivity to monovalent cation. The design of this mutation was inspired by actin and the structure is more suggestive of actin, than of Hsc70. The non-native ϵ-amino nitrogen is much closer to the position of that of actin's lysine 18. In addition, the mutant side chain's contacts with the α-phosphate of bound nucleotide (Figure 5) and with residue T37 are similar to those seen in actin. The functional similarity of the Hsc70 replacement C17K to actin lysine 18 is difficult to assess as soluble actin (the form found in crystals) has no significant ATPase activity. Actin's potential ATPase rate, that measured for polymerized actin [0.07 s^{-1}, (*21*)], is similar to that of the Hsc70 ATPase fragment.

The D206K mutant lysine appears to be an excellent structural mimic of the potassium ion bound in the wild-type structure. The X-ray crystallographic structure of D206K shows that the introduced ϵ-amino nitrogen occupies the position (within the 0.3 Å accuracy of the structure) of the site 2 potassium ion. It is worth noting that it occupies a significantly different position from that of sodium at this site. Nonetheless, the mutant shows activity much more like wild-type protein in the presence of sodium rather than potassium. Two possible explanations suggest themselves.

The first explanation holds that while the potassium ion has been replaced, the carboxylate of aspartic acid 206 has been lost along with its negative charge. The hydrolytic rate may be sensitive to this change. It is relevant to note that mutations K71A, K71M, and K71E resulted in a third potassium ion bound in the active site, possibly to compensate for the loss of the positive charge of the lysine side chain in the mutants (*22*). Additionally, D199S maintains net charge by loss of the potassium ion at site 2 (D.B.M. and Eric R. Johnson, unpublished observation).

The second explanation suggests that the ϵ-amino nitrogen may not have sufficient freedom of motion. A model of the hydrolytic mechanism based on structures of w.t. Hsc70 bound to substrate, substrate analogue, and products requires the γ-PO_4 to move 3−4 Å to access the transition state, with concomitant rearrangement of active site solvent molecules (*23*). Indeed, the γ-PO_4 has been observed in different positions in different crystal structures (*22*). Flexibility may be necessary at site 2 with the potassium ion traveling a path to the transition state which the lysine side chain cannot follow.

The hydrolytic rate constants measured here include both bond cleavage and any rearrangement occurring between binding and cleavage. The kinetic constants of any such a conformational shift in the ATPase domain have not been experimentally accessible in the w.t. protein: the w.t. isolated ATPase fragment has not been shown to undergo such a shift in solution. However, full-length Hsc70 shows a potassium/ATP-dependent conformational shift (*3, 24*). After binding nucleotide but before hydrolysis, full-length Hsc70 assumes a compact conformation with a time constant on the order of seconds (*24*). Our experiments cannot distinguish whether such a step occurs in the isolated ATPase domain, only that the steps after binding which culminate in phosphoryl transfer are, in aggregate, much slower in these mutant proteins.

These results support the fastidious requirement of the hydrolytic activity for precise size, position, and electrostatic character of the bound potassium ion at both sites. The requirement for potassium rather than sodium reveals the same delicate tolerance. In addition, previous studies have shown that modest changes in active site side chains (e.g., asparagine to aspartic acid or glutamine to glutamic acid) consistently lead to only modest structural changes but significant decreases in hydrolytic activity (*23*, *13*). The strict requirements for ion size and position are consistent with its roles in positioning the transferred phosphate and deshielding the phosphorus atom in preparation for nucleophilic attack, roles proposed for potassium ions in this enzyme (*5*) and in fructose-1,6-bisphosphatase (*25*).

The impaired catalytic capacity of these mutants emphasizes the sensitivity of the Hsc70 ATPase site to small changes and the importance of its bound potassium ions. The tight nucleotide binding, informed by the crystal structures of these mutant ATPase domains, suggests that an ion-replacement strategy can succeed where binding alone is of interest.

ACKNOWLEDGMENT

We thank Kevin Flaherty for assistance in X-ray data collection and reduction, Dr. Jeung-Hoi Ha for the gift of [α-^{32}P]ADP, and Samina Taha for assistance in cloning and protein purification.

REFERENCES

1. Chappell, T. G., Konforti, B. B., Schmid, S. L., and Rothman, J. E. (1987) *J. Biol. Chem. 262*, 746−751.
2. Gragerov, A., Zeng, L., Zhao, X., Burkholder, W., and Gottesman, M. E. (1994) *J. Mol. Biol. 235*, 848−854.
3. Palleros, D. R., Reid, K. L., Shi, L., Welch, W. J., and Fink, A. L. (1993) *Nature 365*, 664−666.
4. O'Brien, M. C., and McKay, D. B. (1995) *J. Biol. Chem. 270*, 2247−2250.
5. Wilbanks, S. M., and McKay, D. B. (1995) *J. Biol. Chem. 270*, 2251−2257.
6. Suelter, C. H. (1970) *Science 168*, 789−795.
7. Larsen, T. M., Benning, M. M., Wesenberg, G. E., Rayment, I., and Reed, G. H. (1997) *Arch. Biochem. Biophys. 345*, 199−206.
8. Villeret, V., Huang, S., Fromm, H. J., and Lipscomb, W. N. (1995) *Proc. Natl. Acad. Sci. U.S.A. 92*, 8916−8920.
9. Laughlin, L. T., and Reed, G. H. (1997) *Arch. Biochem. Biophys. 348*, 262−267.
10. Pauling, L. (1948) *The Nature of the Chemical Bond*, p 350, Cornell University Press, Ithaca, NY.
11. Kabsch, W., Mannherz, H. G., Suck, D., Pai, E. F., and Holmes, K. C. (1990) *Nature 347*, 37−44.
12. Flaherty, K. M., McKay, D. B., Kabsch, W., and Holmes, K. C. (1991) *Proc. Natl. Acad. Sci. U.S.A. 88*, 5041−5045.
13. Wilbanks, S. M., DeLuca-Flaherty, C., and McKay, D. B. (1994) *J. Biol. Chem. 269*, 12893−12898.
14. O'Brien, M. C., and McKay, D. B. (1993) *J. Biol. Chem. 268*, 24323−24329.
15. Ha, J.-H., and McKay, D. B. (1994) *Biochemistry 33*, 14625−14635.
16. DeLuca-Flaherty, C., Flaherty, K. M., McIntosh, L. J., Bahrami, B., and McKay, D. B. (1988) *J. Mol. Biol. 200*, 749−750.
17. Otwinowski, Z. (1990) *DENZO Data Processing Package*, Yale University, New Haven, CT.
18. CCP4 (1994) *Acta Crystallogr. D50*, 760−763.
19. Brunger, A. T., Kuriyan, J., and Karplus, M. (1987) *Science 235*, 458−460.
20. Jones, T. A., and Thirup, S. (1986) *EMBO J. 5*, 819−822.
21. Pollard, T. D., and Weeds, A. G. (1984) *FEBS Lett 170*, 94−98.
22. O'Brien, M. C., Flaherty, K. M., and McKay, D. B. (1996) *J. Biol. Chem. 271*, 15874−15878.
23. Flaherty, K. M., Wilbanks, S. M., DeLuca-Flaherty, C., and McKay, D. B. (1994) *J. Biol. Chem. 269*, 12899−12907.
24. Wilbanks, S. M., Chen, L., Tsuruta, H., Hodgson, K. O., and McKay, D. B. (1995) *Biochemistry 34*, 12095−12106.
25. Zhang, R., Villeret, V., Lipscomb, W. N., and Fromm, H. J. (1996) *Biochemistry 35*, 3038−43.
26. Kraulis, P. (1991) *J. Appl. Crystallogr. 24*, 946−950.

BI973046M